On the Shape and Stability of a Drop on a Solid Surface

Gersh O. Berim and Eli Ruckenstein*

Department of Chemical and Biological Engineering, State University of New York at Buffalo, Buffalo, New York 14260

Received: May 3, 2004; In Final Form: July 7, 2004

The shape and stability of a liquid drop on a bare planar solid surface are analyzed by minimizing its total potential energy calculated microscopically. The solution of the obtained differential equation for the drop profile shows that there is a rapid variation of the angle between the tangent to the profile and the solid surface in the region near the leading edge. At the leading edge, this angle is equal to 180° and is independent of the interaction parameters and drop size. For a large droplet, the profile of which is close to a circular one everywhere except in the microscopically small region near the solid surface, a macroscopic contact angle θ_m is introduced, which is identified as the experimentally measured contact angle. The following simple expression was derived for this angle: $\cos\theta_m = (a - 2)/2$, where a depends on the microscopic parameters of the intermolecular interactions (see section III.D for details). For cylindrical droplets, an analytical criterion was found that connects the droplet stability to the parameters involved in the interaction potentials. Two different domains of stability were identified. In the first one, a liquid droplet is stable for any height, y_m, defined as the distance of its apex from the solid surface. The drop profile of large drops sufficiently far from the solid surface is close to circular with a rapid variation of curvature near the solid surface. In the second domain, the drop height y_m is limited by a critical value $y_{m,c}$. If y_m is close to but less than $y_{m,c}$, the drop has a planar shape. If $y_m > y_{m,c}$, no drop can exist. Similar features were established numerically for axisymmetrical drops and compared to those of cylindrical drops.

I. Introduction

The study of the shape of a drop on a solid substrate[1−7] was motivated by the existence of numerous cases in which the shape plays a significant role. As examples, one can mention heterogeneous nucleation,[8,9] supported metal catalysts,[10] and the roll-up transition on cylindrical surfaces.[7]

Most of the mentioned studies are based on thermodynamic considerations applied to large droplets and involved such macroscopic parameters as the pressure and the surface and line tensions. The drop was usually considered as a continuum medium of constant density, and the differential equation of the drop profile has been obtained from the minimum of the calculated macroscopic free energy of the drop.[3,5−7] Two main regimes have been considered, which correspond to (i) a bare surface[2,6] and (ii) one covered with a thin liquid film.[5,6] Among the obtained results, let us note an expression for the microcontact angle θ between the drop surface and the bare solid surface at the leading edge of the drop[6]

$$\cos\theta = 1 + \frac{S - P(0)}{\gamma} \tag{1}$$

where $S = \gamma_{SG} - \gamma_{SL} - \gamma$ is the spreading coefficient, γ_{SG} and γ_{SL} are the surface free energies of the solid/gas and solid/liquid interfaces, γ is the liquid/gas surface tension, and $P(0)$ is the potential solid/liquid interaction energy near the bare surface of the solid. This expression provides a stability condition for a drop, which involves the macroscopic parameters of interaction of the liquid with the environment. A drop exists only if $|1 + (S - P(0))/\gamma| \leq 1$.

It is a challenging problem to describe the drop shape and the contact angle from the point of view of a microscopic theory that uses only the potentials of the intermolecular interactions. A first microscopic approach to investigate the droplet shape, which took into account the liquid−liquid and liquid−solid interactions, was developed by Ruckenstein and Lee.[1] Using the condition of zero tangential force on the surface of a drop in equilibrium and realistic interaction potentials, they obtained an integral equation that can provide the shape of a droplet on a bare surface. From the analysis of that equation, the possibilities of a planar shape of a droplet and of a rapid variation of the direction of the tangent to the profile in the close vicinity of the leading edge were predicted. The analysis of the contact angle provided a condition for the droplet stability.

In the present paper, the investigation of the problem on the basis of a microscopic approach is continued. The shape of a drop on a bare planar solid surface is obtained by minimizing the total potential energy of the drop and neglecting for simplicity the effect of the entropy. In section II, the intermolecular interactions are defined and the total potential energy of a drop is calculated in a general form. Instead of an integral equation, a simpler differential equation for the droplet profile, which is similar to the augmented Young−Laplace equation,[6] is derived for cylindrical (section III) and axisymmetrical (section IV) homogeneous droplets. From the general conditions that the apex of the droplet should be located on the symmetry axis of the profile and the leading edge located on the solid surface, the microcontact angle θ between a drop and the solid surface could be determined to be equal to 180°, hence

* To whom correspondence should be addressed. Electronic mail: feaeliru@acsu.buffalo.edu. Phone number: (716)645-2911, ext. 2214. Fax: (716)645-3822.

10.1021/jp048093k CCC: $27.50
Published on Web 11/19/2004

independent of the interaction parameters. It was shown that the change of the profile slope from an acute angle to 180° occurs in the very vicinity of the leading edge of a large drop, a region that is not observable in macroscopic experiments. An observable macroscopic contact angle θ_m was introduced and calculated for a large droplet using a continuation of the circular part of its profile. As expected that angle did depend on the interaction parameters. A condition for the stability of the droplets was found that was derived from the analysis of the existence of a solution of the differential equation for the droplet profile. From this condition, two ranges of values of the interaction parameters were found in which the droplet can have any height or the height y_m is limited by a critical value $y_{m,c}$ and a stable droplet with a height larger than $y_{m,c}$ cannot exist. The critical height $y_{m,c}$ depends on the parameters that characterize the interaction potentials. One should note that the expressions for the contact angles θ and θ_m were not involved in the determination of the stability condition.

II. Formulation of the Problem and Basic Equations

A. The Potentials. A molecule of a liquid drop immersed in its vapor and located on the bare solid surface interacts with the other molecules of the drop with an interaction potential ϕ_{LL}, with the molecules of vapor with a potential ϕ_{LV}, and with the molecules of the solid with a potential ϕ_{LS}. At equilibrium, a drop acquires the shape which for a given volume V minimizes its free energy. Because the contact angle is weakly dependent upon temperature, one can neglect the role of entropy and minimize only the total potential energy of the droplet. Below it will be assumed that the interaction of the drop molecules with the vapor molecules is negligible. The interaction potential, $\phi_{LL}(r)$, between two molecules of liquid the centers of which are separated by a distance r is assumed to be of the simplest, square-well form

$$\phi_{LL}(r) = \begin{cases} -\epsilon_{LL} & r \le \eta \\ 0 & r > \eta \end{cases} \tag{2}$$

where η is the radius of interaction and ϵ_{LL} characterizes the strength of the interaction. Despite its oversimplified form, such a potential was used as a reasonable approximation for the qualitative understanding of various phenomena.[11]

The interaction potential ϕ_{LS} between the molecules of liquid and solid is chosen by combining the London−van der Waals attraction with a rigid core repulsion

$$\phi_{LS}(r) = \begin{cases} -\epsilon_{LS}\left(\frac{\sigma}{r}\right)^6 & r \ge \sigma \\ \infty & r < \sigma \end{cases} \tag{3}$$

where σ and $\epsilon_{LS} > 0$ are the size of the repulsive core and the interaction constant, respectively. Below σ is used as a unit of length, and for numerical estimations, the value $\sigma \simeq 3.4$ Å was selected.[12]

B. Liquid−Solid Interaction. Assuming pairwise additivity, the interaction potential of a molecule of liquid with a semi-infinite solid can be written as

$$\Phi(y) = -\frac{1}{6}\pi\epsilon_{LS}\rho_S\sigma^3\left(\frac{\sigma}{\sigma + y}\right)^3, \quad y \ge 0 \tag{4}$$

where $\sigma + y$ is the distance of the center of a molecule of liquid from the center of the first layer of solid atoms and ρ_S is the (constant) number density of molecules in the solid. The total potential energy, U_{LS}, associated with the liquid−solid interactions is given by

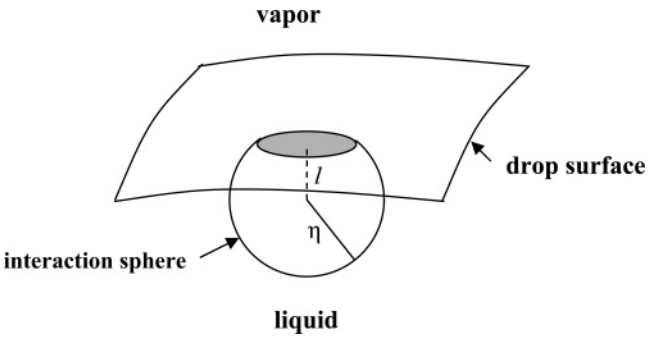

Figure 1. Interaction range of a molecule near the surface of a drop ($l < \eta$). If the drop surface has a radius of curvature much larger than η, the intersection of the interaction sphere with the drop can be considered planar.

$$U_{LS} = \int_V \rho_L \Phi(y)\, dV \tag{5}$$

where V is the volume of the droplet.

C. Liquid−Liquid Interaction. Let us assume that the size of the droplet is much larger than the radius η of the range of liquid−liquid interactions. Then a molecule of liquid at a distance larger than η from the droplet surface interacts with all the molecules inside a sphere of radius η and the center in the center of the molecule (interaction sphere). The effective potential of this molecule is proportional to the number of molecules inside the sphere and is equal to

$$\phi_1 = -\frac{4}{3}\pi\eta^3\rho_L\epsilon_{LL} \tag{6}$$

where ρ_L is the number density of molecules in the liquid, which is considered constant.

A molecule at a distance $l < \eta$ from the droplet surface interacts only with those molecules that are present both in the drop and in the interaction sphere described above (Figure 1). Assuming that the radius of curvature of the surface is much larger than η, one can consider the intersection of the interaction sphere with the drop to be planar. (Such an assumption is valid if the drop volume V is much larger than the volume of the interaction sphere, $V \gg {}^4/_3\pi\eta^3$.) In this case, the effective potential $\phi_2(l)$ of a molecule near the drop surface is

$$\phi_2(l) = -\pi\epsilon_{LL}\rho_L\int_{-\eta}^{l}(\eta^2 - z^2)\, dz = -\frac{2}{3}\pi\eta^3\epsilon_{LL}\rho_L\left[1 + \frac{3}{2}\frac{l}{\eta} - \frac{1}{2}\left(\frac{l}{\eta}\right)^3\right] \quad (l \le \eta) \tag{7}$$

On a schematic representation of a drop having an arbitrary shape (see Figure 2), the dashed line separates the volume V_1 in which each molecule has the effective potential eq 6 from the volume V_2 in which eq 7 is valid. After integration over the volume V_1, one obtains for the total potential energy U_1 of molecules in this volume

$$U_1 = \frac{1}{2}\phi_1\rho_L V_1 = -\frac{2}{3}\pi\eta^3\rho_L{}^2\epsilon_{LL}V_1 \tag{8}$$

where the factor ${}^1/_2$ avoids the double counting of the interaction energy during integration.

To calculate the energy U_2 of all molecules in the volume V_2, let us first find the energy dU_2 of the molecules in the cylindrical volume dV_2 with the base area ds and height η normal

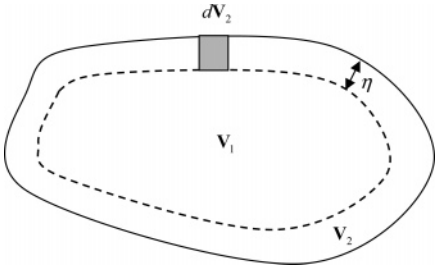

Figure 2. Cross-sections of a drop surface (—) and of the surface located at a distance η from the drop surface (— — —). Inside the volume V_1, any molecule interacts with all the molecules inside the interaction sphere with the center in the center of the selected molecule. The elementary volume dV_2 has the base area ds and height η.

to the surface (Figure 2)

$$dU_2 = \frac{1}{2} ds\rho_L \int_0^\eta \phi_2(l)\, dl = -\frac{13}{24}\pi\eta^4\epsilon_{LL}\rho_L{}^2\, ds \qquad (9)$$

Then the energy U_2 can be written as follows:

$$U_2 = -\frac{13}{24}\pi\eta^4\epsilon_{LL}\rho_L{}^2 S \qquad (10)$$

where $S = S_{LV} + S_{LS}$, S_{LV} (S_{LS}) being the area of the interface between the droplet and vapor (solid). When the approximation $V_2 = S\eta$ is used for the volume V_2, the total potential energy $U_{LL} = U_1 + U_2$ of the droplet associated with the liquid−liquid interactions can be written as

$$U_{LL} = -\frac{2}{3}\pi\eta^3\rho_L{}^2\epsilon_{LL}V + \frac{1}{8}\pi\eta^4\rho_L{}^2\epsilon_{LL}S \qquad (11)$$

The two terms in eq 11 represent the bulk and surface energy of the droplet, and the coefficient multiplying the area S provides a microscopic expression for the surface tension γ_L of the liquid

$$\gamma_L = \frac{1}{8}\pi\eta^4\rho_L{}^2\epsilon_{LL} \qquad (12)$$

The total droplet energy U_{total} is given by

$$U_{total} = U_{LL} + U_{LS} = -\frac{2}{3}\pi\eta^3\rho_L{}^2\epsilon_{LL}V + \frac{1}{8}\pi\eta^4\rho_L{}^2\epsilon_{LL}S - \frac{\pi}{6}\epsilon_{LS}\rho_S\rho_L\sigma^3\int_V\left(\frac{\sigma}{\sigma+y}\right)^3 dV \qquad (13)$$

One should note that the total potential energy (eq 13) does not include the gravitational and liquid−vapor contributions, which are considered small.

In the following sections, the shape of the drop will be examined for cylindrical and axisymmetrical drops.

III. Cylindrical Droplet

A. An Equation for the Profile. Let us consider a cylindrical liquid drop on a smooth bare solid surface *XOZ*, extended along the *z*-axis and with a cross-section symmetrical with respect to the *y*-axis (Figure 3). Usually one assumes[5,6] that the micro-contact angle θ, that is, the angle between the drop surface and the solid surface at the leading edge of the drop, is less than 90° and that the droplet has a bell-like shape (Figure 3a). In this case, the equation of the profile can be chosen in the form $y = y(x)$ where $y(x)$ satisfies an equation of the form $f(x,y,(dy/dx),(d^2y/dx^2)) = 0$ for the entire profile. However, if the drop has the shape presented in Figure 3b with $\theta > 90°$, then the above equation is no longer valid due to the lack of uniqueness of the function $y = y(x)$ for $|x| > x_0$, where x_0 is the abscissa of the leading edge of the droplet. To avoid this difficulty and include both shapes (Figure 3 parts a and b), the equation for the droplet profile will be written in the form $x = x(y)$ and only that part of the profile for which $x \geq 0$ will be considered. The volume V of the drop, the areas of the liquid−vapor (S_{LV}), and liquid−solid (S_{LS}) interfaces, and $\int_V(\sigma^3/(\sigma+y)^3)\, dV$ are given by

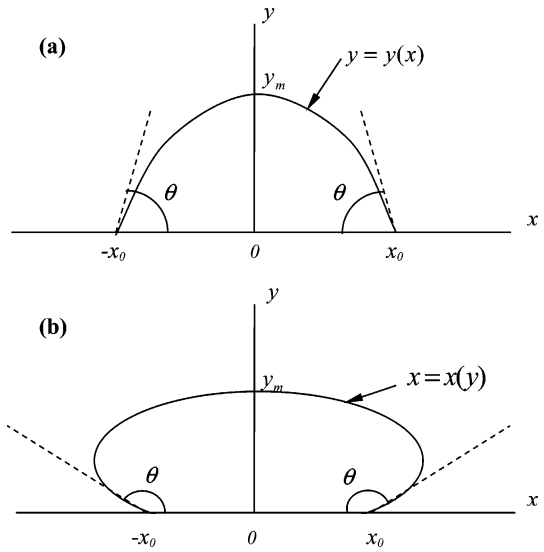

Figure 3. Two characteristic profiles of a cylindrical droplet: (a) the contact angle θ at the leading edge of the droplet is less than 90°; (b) the same angle is larger than 90°. The *z*-axis is normal to the plane of the figure.

$$V = 2\int_0^{y_m} x(y)\, dy$$

$$S_{LV} = 2\int_0^{y_m}\sqrt{1 + x_y{}^2}\, dy$$

$$S_{LS} = 2x(0)$$

$$\int_V \frac{\sigma^3}{(\sigma+y)^3}\, dV = 2\int_0^{y_m} x\frac{\sigma^3}{(\sigma+y)^3}\, dy \qquad (14)$$

where y_m is the largest ordinate of the droplet profile (the height of the droplet) and the subscript y denotes the derivative with respect to y. All the quantities in eq 14 are given per unit length of the droplet in the *z* direction.

With the use of the identity $x(0) = -\int_0^{y_m} x_y\, dy$, which follows from $x(y_m) = 0$, the total potential energy eq 13 per unit length becomes

$$U_{total} = \int_0^{y_m} f(y,x,x_y)\, dy \qquad (15)$$

where

$$f(y,x,x_y) = \frac{1}{4}\pi\eta^4\rho_L{}^2\epsilon_{LL}[-a_0 x + \sqrt{1 + x_y{}^2} - x_y - ax\phi(y)] \qquad (16)$$

and

$$a_0 = \frac{16}{3\eta}, \quad a = \frac{4}{3}\frac{\epsilon_{LS}}{\epsilon_{LL}}\frac{\rho_S}{\rho_L}\left(\frac{\sigma}{\eta}\right)^4, \quad \phi(y) = \frac{\sigma^2}{(\sigma+y)^3} \qquad (17)$$

The actual drop profile has to minimize the total potential energy of the drop for a given drop volume. The problem is thus

reduced to the minimization of the functional

$$v[x(y)] = \int_0^{y_m} F(y,x,x_y)\, dy \tag{18}$$

where

$$F(y,x,x_y) = \lambda_c x + \sqrt{1 + x_y^2} - x_y - ax\phi(y) \tag{19}$$

and λ_c is a Lagrange multiplier for the drop volume.

The standard calculus of variations[13] provides the following differential equation for the profile:

$$\frac{x_{yy}}{(1 + x_y^2)^{3/2}} + a\phi(y) - \lambda_c = 0 \tag{20}$$

where the first term has the meaning of a curvature $\kappa(y)$ of the profile. This equation has to be complemented with the so-called transversality conditions[13]

$$\frac{\partial}{\partial x_y} F(y,x,x_y)|_{y=0} = 0, \quad \left[F(y,x,x_y) - x_y \frac{\partial}{\partial x_y} F(y,x,x_y)\right]|_{y=y_m} = 0 \tag{21}$$

which reflect the fact that the ends of the considered part of the profile ($x \geq 0$) should be located on the x (contact point with the solid) and y (drop apex) axes. In the considered case, these conditions have the forms

$$\frac{x_y}{\sqrt{1 + x_y^2}}|_{y=0} = 1 \tag{22}$$

and

$$\frac{1}{\sqrt{1 + x_y^2}}|_{y=y_m} = 0 \tag{23}$$

The left-hand side of eq 22 is equal to $-\cos\theta$, where θ is the microcontact angle of the drop on the solid surface (Figure 3b). Therefore condition 22 provides $\theta = 180°$ between the droplet and the solid, independent of the parameters of the model. One should note that at the point of contact the derivative x_y diverges ($x_y|_{y=0} = \infty$). The second transversality condition, eq 23, can be replaced by

$$x_y|_{y=y_m} = \infty \tag{24}$$

or, equivalently, by $y_x|_{x=0} = 0$, and is a consequence of the symmetry of the drop profile with respect to the y-axis.

Denoting $p(y) = x_y$, one can transform eq 20 into a first-order equation

$$\frac{p_y}{(1 + p^2)^{3/2}} = \lambda_c - a\phi(y) \tag{25}$$

with the solution

$$p = \frac{\Psi(y)}{\sqrt{1 - \Psi^2(y)}} \tag{26}$$

where

$$\Psi(y) = \lambda_c y + \frac{a\sigma^2}{2(\sigma + y)^2} + C \tag{27}$$

and C is a constant. Substituting $p = x_y$ into eq 26, one can obtain a final general solution for $x(y)$ in the form

$$x(y) - x(0) = \int_0^y \frac{\Psi(y)}{\sqrt{1 - \Psi^2(y)}}\, dy \tag{28}$$

The point of contact $x(0) = x_0$ is given by

$$x(0) = -\int_0^{y_m} \frac{\Psi(y)}{\sqrt{1 - \Psi^2(y)}}\, dy \tag{29}$$

which follows from eq 28 and the condition $x(y_m) = 0$.

The solution 28 contains three unknown quantities, namely, the constant of integration C, the Lagrange multiplier λ_c, and the height of the droplet y_m, which have to be found using suitable constraints. First of these constraints is provided by the transversality condition 22, which is equivalent to the equation $\Psi(0) = 1$ and which gives for C the value $C = 1 - a/2$. As a result, function $\Psi(y)$ becomes

$$\Psi(y) = 1 - \frac{a}{2} + \lambda_c y + \frac{a\sigma^2}{2(\sigma + y)^2} \tag{30}$$

The second transversality condition, provided by eq 24, and eq 26 together with the definition of p lead to $\Psi(y_m) = \pm 1$. To select the correct sign, one should take into account that in the limit $a \to 0$, that is, in the absence of liquid−solid interactions, the profile has to be circular. To recover such a result from eq 26, one has to select $\Psi(y_m) = -1$. Obviously, the same sign is also valid when $a \neq 0$, and this provides a relation between y_m and λ_c

$$\lambda_c = \frac{1}{y_m}\left[-2 + a/2 - \frac{a\sigma^2}{2(\sigma + y_m)^2}\right] \tag{31}$$

which follows from eq 30 at $y = y_m$. Finally, one has the condition of fixed volume ($V = 2\int_0^{y_m} x\, dy = \text{const}$), which after integration by parts and employing eq 26 and condition $x(y_m) = 0$ can be rewritten in the form

$$V = -2\int_0^{y_m} \frac{y\Psi(y)}{\sqrt{1 - \Psi^2(y)}}\, dy \tag{32}$$

Equation 32 together with eqs 30 and 31 allows one to find the unknown parameters λ_c, y_m, and $x(0)$ and hence to find the shape of the droplet. Even though the detailed profile can be obtained only numerically, eqs 20 and 28 allow one to extract some general conclusions. Thus, eq 20 shows that the curvature of the profile is equal to $\kappa(y) = \lambda_c - a\phi(y)$, where $\phi(y)$ is given by eq 17. The latter function vanishes for $y \gg \sigma$. Consequently, for $y/\sigma \gg 1$, the curvature of the profile is almost constant and equal to λ_c, that is, the shape of that part of the drop can be represented by a circle of radius $R \simeq |1/\lambda_c|$. The question how large is this part can be answered only on the basis of the complete solution of eq 20, and this issue will be examined in the next section.

Equation 28 has a solution only if $|\Psi(y)| < 1$ for $0 < y < y_m$. Because, as noted above, $\Psi(y)$ acquires for $y = y_m$ its smallest value equal to -1, this function has to decrease in the vicinity of y_m and its derivative

$$\frac{d\Psi(y)}{dy} = \lambda_c - \frac{a\sigma^2}{(\sigma + y)^3} \tag{33}$$

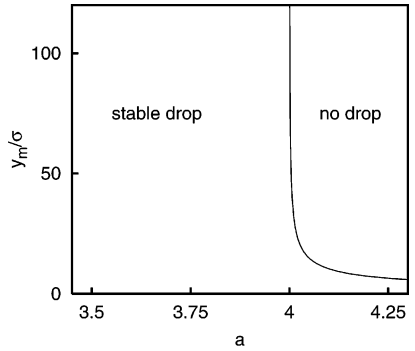

Figure 4. Domains of drop stability in the $a-(y_m/\sigma)$ plane. The solid line provides the critical height $y_{m,c}$ as a function of a. The critical height $y_{m,c}$ increases as a decreases and approaches infinity when $a \rightarrow 4$.

has to be negative at $y = y_m$. Therefore,

$$\lambda_c - \frac{a\sigma^2}{(\sigma + y_m)^3} < 0 \tag{34}$$

The latter inequality together with the explicit expression for λ_c given by eq 31 provides the following inequality between the parameter a and the droplet height y_m:

$$a < 4\left(\frac{\sigma}{y_m}\right)^2 \frac{(1 + y_m/\sigma)^3}{3 + y_m/\sigma} \tag{35}$$

Condition 35 for the existence of a solution to eq 20 for the drop profile consitutes a necessary stability condition for the droplet, which will be examined in more detail in section III.B.

Eq 20 has the same form as the augmented Young−Laplace equation[6]

$$\frac{y_{xx}}{(1 + y_x^2)^{3/2}} + \Pi(y)/\gamma_L = -p_c/\gamma_L \tag{36}$$

for the drop profile given as a function of x [$y = y(x)$], which is applicable to drop shapes as in Figure 3a. Here γ_L is the bulk liquid/gas surface tension, $\Pi(y)$ is the disjoining pressure, and p_c is the capillary pressure. Because the first terms of eqs 36 and 20 represent the profile curvature, one can establish the folowing correspondence between the macroscopic parameters of eq 36 and the microscopic parameters of eq 20: $p_c/\gamma_L = -\lambda_c$; $\Pi(y)/\gamma_L = a\phi(y)$.

B. Stability of the Drop. As mentioned above, the equation for the droplet profile has a solution only if the parameter a and the droplet height y_m satisfy inequality 35. The examination of that inequality shows that for $a > 4$ a solution exists only when the height of the droplet, y_m, is smaller than a critical value $y_{m,c}$ provided by the equation

$$\left(\frac{\sigma}{y_{m,c}}\right)^2 \frac{(1 + y_{m,c}/\sigma)^3}{3 + y_{m,c}/\sigma} = \frac{a}{4} \tag{37}$$

The dependence of $y_{m,c}$ on a is given by the solid line of Figure 4. The solid line separates two regions; in one, at the right, droplets cannot exist, while in the other, at the left, droplets do exist. If $a \rightarrow 4$, $y_{m,c}$ grows to infinity. For $a < 4$, droplets of any height can exist.

C. Shape of the Drop. A typical profile of a cylindrical droplet for $a < 4$ ($a = 2.5$) is presented in Figure 5 for two

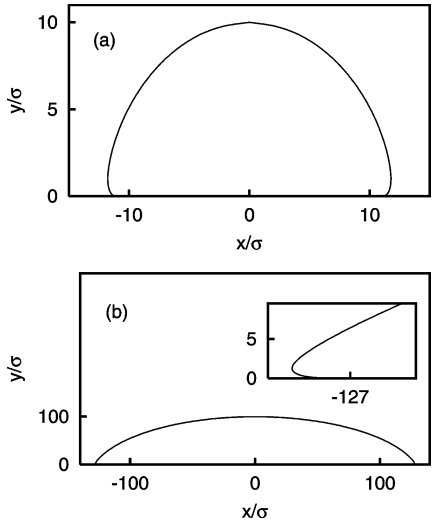

Figure 5. Profiles of droplets of different volumes for $a = 2.5$: (a) small droplet with $V/\sigma^3 \simeq 183.5$, $y_m/\sigma = 10$; (b) large droplet with $V/\sigma^3 \simeq 1.9 \times 10^4$, $y_m/\sigma = 100$. On both figures, the shape of the drop near the leading edge is similar to that shown in the insert.

different drop volumes, a relatively small volume ($V/\sigma^3 = 183.5$, $y_m/\sigma = 10$) and a relatively large one ($V/\sigma^3 = 1.9 \times 10^4$, $y_m/\sigma = 100$). In both cases, the microcontact angle is equal to 180°, and near the leading edge, there is a rapid variation of the profile curvature as well as of the angle between the tangent to the profile and the solid surface (see insert in Figure 5b).

The traditional approximation of the profile of a drop on a plane surface is to consider it as a part of a circle.[4,9] If the height of the drop (y_m) and the radius R of the circle are known, then one can easily calculate the drop volume and the areas of the interfaces. If the approximation of the drop profile by a circle is valid, then the radius of curvature will be the same at any (or almost any) point of the profile. To verify its validity in the framework of the present microscopic approach, we calculated the radius of curvature, $R^{curv}(y)$, of the profile as a function of the distance y from the solid surface for several values of the droplet height y_m, using the expression

$$R^{curv}(y) \equiv \left|\frac{1}{\kappa(y)}\right| = \left|\lambda_c - \frac{a\sigma^2}{(\sigma + y)^3}\right|^{-1} \tag{38}$$

which was obtained from the definition of the radius of curvature and eq 20. In Figure 6, this dependence is presented for several values of y_m by plotting the normalized coordinate $R^{curv}(y)/R_m^{curv}$ vs y/y_m, where $R_m^{curv} \equiv R^{curv}(y_m)$ is the largest value of the curvature radius, which the profile has at the drop apex ($y = y_m$, $x = 0$). The parameter a was selected smaller than 4 ($a = 3$) to allow for the existence of droplets of any size. One can see that for small droplets ($y_m/\sigma = 10$), there is no range in which the radius of curvature is constant. For such droplets, the profile cannot be approximated by a circle. However, for large drops, $y_m/\sigma = 1000$, the radius of curvature for $y > 0.1y_m$ is almost equal to its largest value ($R_m^{curv}/\sigma = 2000.0$) and the profile can be considered as a part of a circle. Numerical analysis shows that for $a < 4$ the radius R of that circle is proportional to the height of the droplet y_m ($R = ky_m$). The proportionality coefficient k is a function of a and, for example, for $a = 3$, $k = 2$. The approximation by a circle is valid starting from $y_m/\sigma \simeq 100$.

In Figure 7, a similar plot, but for $a = 4.01$, is presented. For this value of a, the height of the drop cannot exceed the

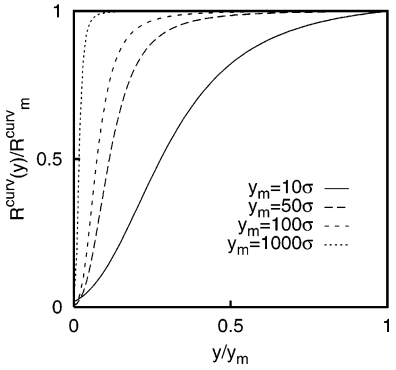

Figure 6. Radius of the profile curvature for droplets of various sizes for $a < 4$ ($a = 3$). For a relatively large droplet ($y_m/\sigma = 100$), the curvature radius is almost constant for $y > 0.1y_m$. R_m^{curv}/σ is equal to 18.7, 99.7, 199.8, and 2000.0 for y_m/σ equal to 10, 50, 100, and 1000, respectively.

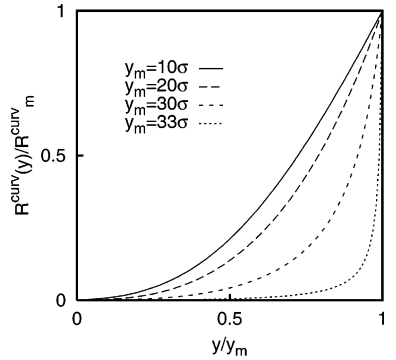

Figure 7. The radius of the profile curvature for droplets of various sizes for $a > 4$ ($a = 4.01$). R_m^{curv}/σ is equal to 240.0, 2437.0, 2.67×10^3, and 3.26×10^5 for y_m/σ equal to 10, 20, 30, and 33, respectively.

critical value $y_{m,c}/\sigma = 33.34$, and there is no range in which $R^{curv}(y)$ of the profile is constant. Therefore for this case, the approximation by a circle is not at all valid. For a height y_m of the droplet close to the critical one ($y_m/\sigma = 33$), the curvature radius for $y > 0.9y_m$ is much larger than y_m ($R_m^{curv}/y_m \approx 10^4$), and the width of the droplet, $2x(0)$, is much larger than the height ($2x(0)/y_m \simeq 100$). The shape of the droplet can be considered to be planar in this range.

D. Contact Angle. As shown in section III.A, the microcontact angle θ of a drop on the bare surface at the leading edge is always equal to 180°, independent of the intermolecular interactions. This is in apparent contradiction with the experimental results, which provide for θ a variety of values (see, for example, ref 14). To resolve this contradiction, one should note that the measurements of the contact angles were performed for large drops ($y_m > 1$ μm) for which the main part of the drop profile can be considered circular and the part near the surface of the solid (which is similar to that shown in the insert of Figure 5b), where very rapid curvature changes occur, is extremely small. For such a large drop, it is reasonable to define a macroscopic contact angle, which can be measured in macroscopic experiments, as the angle between the continuation of the circular part of the profile until its intersection with the solid surface (see Figure 9a). In this case, the value θ_m of this angle is given by the simple formula

$$\cos\theta_m = 1 - \frac{y_m}{R_m^{curv}} \tag{39}$$

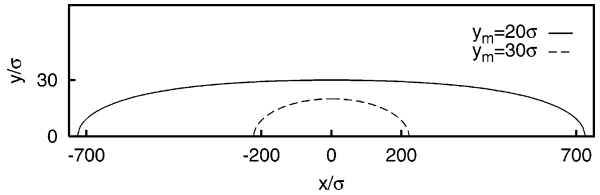

Figure 8. The droplet shape for $a > 4$ ($a = 4.01$) for two values of the droplet height. For the height $y_m/\sigma = 30$ close to the critical value $y_{m,c}/\sigma = 33.34$, the shape is planar, while for smaller heights ($y_m/\sigma = 20$), it has a nonplanar profile.

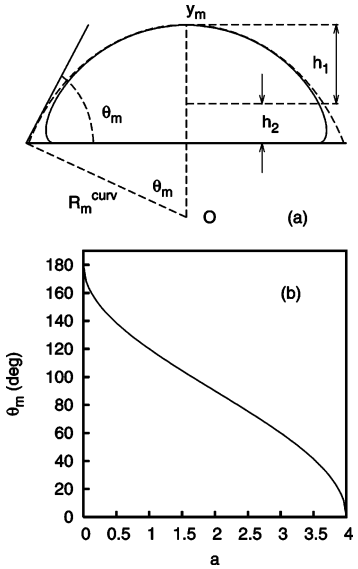

Figure 9. Panel a provides the definition of a macroscopic contact angle θ_m. Here h_1 is the range of constant profile curvature corresponding to the curvature radius R_m^{curv}, y_m is the droplet height, h_2 is the range of rapid change of the profile curvature. It is assumed that $h_2/h_1 \leq 0.1$. Panel b shows the a-dependence of the macroscopic contact angle given by eq 42.

where R_m^{curv} is the curvature radius at the drop apex and y_m is the height of the drop. The curvature radius R_m^{curv} can be obtained from eq 38, where λ_c is given by eq 31. One can see from Figure 4 that stable large droplets can exist only for $a \leq 4$. In this case

$$R_m^{curv} = 2y_m\left[4 - a + a\frac{1 + 3y_m/\sigma}{(1 + y_m/\sigma)^3}\right]^{-1} \tag{40}$$

and eq 39 provides for $\cos\theta_m$ the expression

$$\cos\theta_m = \frac{1}{2}\left[a - 2 + a\frac{1 + 3y_m/\sigma}{(1 + y_m/\sigma)^3}\right] \tag{41}$$

For large droplet, $y_m \gg \sigma$, and eq 41 acquires the very simple form

$$\cos\theta_m \simeq \frac{1}{2}(a - 2) \tag{42}$$

which connects the macroscopic contact angle to the microscopic parameters involved in the definition of a (see eq 17). It follows from eq 42 that the macroscopic contact angle exists only for $0 \leq a \leq 4$. The latter inequality provides for a the same range of values in which a macroscopic droplet can exist as those of section III.B on the stability of droplets. Therefore the simple eq 42 provides a stability condition for large droplets, which is equivalent to that obtained from the condition (eq 35) of

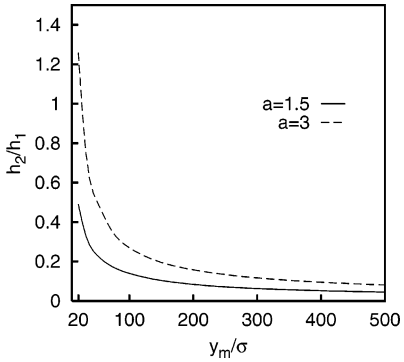

Figure 10. The dependence of the ratio h_2/h_1 characterizing the quality of approximation of a drop profile by a circle on the droplet height for $a = 1.5$ and $a = 3$.

existence of a solution of the differential equation for the drop profile. According to eq 42, a large droplet cannot exist on a bare solid surface for $a > 4$. Once artificially created, it has to spread over the surface to form a planar droplet with a height less than the critical value $y_{m,c}$, similar to those presented in Figure 8.

Note that expressions 41 and 42 can be used if the domain of constant curvature radius of the profile (h_1 in Figure 9a) is much larger than that in which a rapid variation in the profile curvature radius occurs (h_2 in Figure 9a). In the numerical estimations, a radius of curvature was considered constant in the upper part of the profile if its variation within that part did not exceed 5%. The ratio (h_2/h_1) was calculated for several values of a, and the results are presented in Figure 10. One can see that starting from relatively small heights ($y_m = 150\sigma$ for $a = 1.5$ and $y_m = 400\sigma$ for $a = 3$), the above ratio does not exceed 0.1. The larger the droplet height, the smaller is the relative range of rapid variation of the curvature, the size of the range of rapid variation being microscopically small. For example, for a drop with a height $y_m = 400\sigma$ ($\sim$120 nm), this range is equal approximately to 9.9 nm.

One can see from Figure 9b that the macroscopic contact angle increases with decreasing a. To relate this angle to thermodynamic characteristics of the system, one can use the expression for the liquid surface tension γ_L given by eq 12 and the definition of a given by eq 17. Then, θ_m is given by the equation

$$\cos\theta_m \simeq \frac{1}{2}\left(\frac{K}{\gamma_L} - 2\right) \tag{43}$$

where $K = (\pi/6)\epsilon_{LS}\rho_L\rho_S\sigma^4$. From this equation, it follows that for a given solid $\cos\theta_m$ decreases with increasing γ_L, that is, the macroscopic contact angle increases with increasing liquid surface tension. This conclusion is in agreement with experiment (ref 14). One can see from Figures 6 and 7 that the curvature of a small droplet with $y_m < 100\ \sigma$ varies rapidly along the profile. In this case, it is not possible to define a macroscopic contact angle as it was possible for a large droplet.

IV. Axisymmetrical Droplet

This section considers a drop that has a rotational symmetry with respect to the y-axis on a solid surface XOZ. The derivation of the Euler equation for the profile is similar to that for a cylindrical droplet. Instead of eq 14, the following expressions for the volume V and the areas of the interfaces have to be employed

$$V = \pi\int_0^{y_m} x^2\,dy$$

$$S_{LV} = 2\pi\int_0^{y_m} x\sqrt{1 + x_y^2}\,dy$$

$$S_{LS} = \pi x^2(0) = -2\pi\int_0^{y_m} x x_y\,dy$$

$$\int_V \frac{\sigma^3}{(\sigma + y)^3}\,dV = \pi\int_0^{y_m} x^2\frac{\sigma^3}{(\sigma + y)^3}\,dy$$

The total potential energy can be written in the form of eq 15 with

$$f(y,x,x_y) = \frac{\pi^2}{4}\eta^4\rho_L^2\epsilon_{LL}\left[-\frac{a_0}{2}x^2 + x(\sqrt{1 + x_y^2} - x_y) - \frac{a}{2}x^2\phi(y)\right] \tag{44}$$

where $\phi(y)$ is given by eq 17. The Euler equation for the profile becomes

$$\frac{x_{yy}}{(1 + x_y^2)^{3/2}} - \frac{1}{x\sqrt{1 + x_y^2}} + a\phi(y) - 2\lambda_a = 0 \tag{45}$$

where λ_a is a Lagrange multiplier for the drop volume. As for the cylindrical droplet, the transversality conditions 21 can be written in the form

$$x_y|_{y=0} = \infty, \quad x_y|_{y=y_m} = \infty \tag{46}$$

Again, the first condition provides the value $\theta = 180°$ for the microcontact angle, and the second one reflects the fact that the tangent at the drop apex is parallel to the plane of the solid. However, eq 45 cannot be reduced to a first-order differential equation, as for the cylindrical droplet. As a result, it is not possible to formulate analytically, as in section III.A, the necessary condition for the existence of a solution and calculate the drop profile. All the results below were obtained numerically.

A. Stability of the Axisymmetical Drop. As for the cylindrical droplet, there is a critical value, a_c, of the parameter a such that for $a \le a_c$ droplets of any height can exist but for $a > a_c$ the height cannot exceed the (critical) value $y_{m,c}$. Within the precision of the numerical calculations, the value of a_c for axisymmetrical droplets is the same as that for the cylindrical ones, that is, $a_c = 4$. The a-dependence of the critical droplet height $y_{m,c}$ differs, however, somewhat from that for a cylindrical one. One can see from Figure 11 that $y_{m,c}$ for the axisymmetrical droplet is larger than that for the cylindrical one, particularly near the critical value of a.

B. Shape of the Axisymmetrical Drop and Contact Angles. The numerical solution of eq 45 provides the shape of the drop, which is qualitatively similar to that of the cylindrical drop. The cylindrical and axisymmetrical droplets will be compared either for the same height, for the same volume per unit liquid/solid contact area, or for the same volume per unit length of the contact line.

In Figure 12, the profile of an axisymmetrical droplet with the height $y_m/\sigma = 27.0$ and volume $V/\sigma^3 \approx 2 \times 10^5$ (solid curve) is compared with three cylindrical droplets, each of them satisfying one of the above conditions. Only the profiles for $x > 0$ are presented. The difference between the profiles with the same height is small. The profiles have almost the same

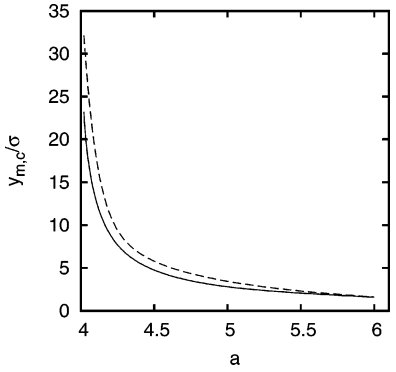

Figure 11. The critical height, $y_{m,c}$, of the axisymmetrical (− − −) and cylindrical (—) droplets as function of a for $a > 4$.

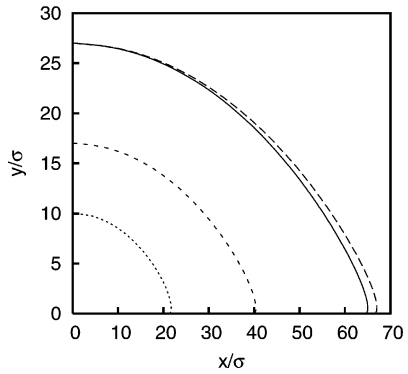

Figure 12. Profile of the axisymmetrical drop (—) and profiles of three cylindrical drops having the same height (− − −), the same volume/(contact area) ratio (•••), and volume/(contact line length) ratio (- - -) as the axisymmetric one.

macroscopic contact angles, $\theta_m = 43.7°$ for the axisymmetrical drop and $\theta_m = 42.0°$ for the cylindrical one. Note that the numerical values of the free terms, $-\lambda_c$ and $-2\lambda_a$, in eqs 20 and 45 for the cylindrical and axisymmetrical profiles, respectively, differ by a factor of $1.86 \simeq 2$, the latter one being the larger. If the height of the drops grows, the above ratio becomes closer to 2. In addition, the difference between the two profiles becomes smaller, and the axisymmetrical profile can be represented by the much simpler eq 20 for the cylindrical drop. One should note that in the considered case the characteristic volume of the cylindrical droplet (per unit length) is equal to $V_{cyl}/\sigma^3 \simeq 2600$, while the volume of the axisymmetrical one, $V_{axis}/\sigma^3 \simeq 2 \times 10^5$, is much larger.

In Figure 12, the profiles of cylindrical drops that have the same volume/(contact area) or volume/(length of the contact line) ratios as the axisymmetrical drop are presented by dashed and dotted lines, respectively. These profiles are lower than that of the axisymmetrical drop but have approximately the same macroscopic contact angles, $\theta_m = 44.8°$ and $\theta_m = 42.7°$, respectively, as the axisymmetrical drop ($\theta_m = 43.7°$).

As for the cylindrical droplet, for $a > 4$, the shape of the axisymmetrical drop becomes planar as the drop height approaches the critical value $y_{m,c}$.

V. Discussion and Conclusion

The analysis provided in sections III and IV for the cylindrical and axisymmetrical drops revealed that their main characteristics are similar. For this reason, the discussion below, if not otherwise mentioned, concerns both kinds of drops.

The interesting result that follows from the microscopic considerations regarding the drop profile is the existence of the stability condition provided by eq 35. This condition, which so far was not noted in the literature, connects the drop stability to the value of a single parameter $a = {}^4/_3(\epsilon_{LS}/\epsilon_{LL})(\rho_S/\rho_L)(\sigma/\eta)^4$, which depends on the microscopic characteristics of the intermolecular interactions. For $a > 4$, the droplet is stable if its height is smaller than a critical height $y_{m,c}$, which depends on a. The critical height increases when a decreases and approaches infinity when $a \rightarrow 4$. For $a \leq 4$, droplets of any height are stable.

One should note that the obtained stability condition does not involve the contact angle θ at the leading edge (microcontact angle), which is constant ($\theta = 180°$). This fact distinguishes it from the stability conditions discussed in refs 1, 4, and 6 and based on the existence of a solution for the contact angle.

Let us note that an unstable state occurs only when the parameter a exceeds the value $a = 4$. Among the quantities contained in this parameter, the most important one is the ratio (σ/η) of the hard core repulsion radius σ of the solid−liquid interactions and the radius η of the liquid−liquid interactions, because $a \approx (\sigma/\eta)$.[4] Only when the ratio σ/η is not too small the ratios $\epsilon_{SL}/\epsilon_{LL}$ and ρ_S/ρ_L, which are also involved in the definition of a, can lead to values of a of the order of 4 required for the drops to become unstable. To evaluate η, let us compare the total potential energy ϕ_1 of a molecule of liquid, given by eq 6, with that provided by the potential

$$\phi'_{LL}(r) = \begin{cases} -\epsilon'_{LL}\left(\dfrac{\sigma_{LL}}{r}\right)^6 & r \geq \sigma_{LL} \\ \infty & r < \sigma_{LL} \end{cases} \quad (47)$$

which is frequently used to describe the intermolecular interactions in liquids. The latter energy of a molecule in the bulk of the liquid is given by

$$\phi'_1 = \int_0^{2\pi} d\phi \int_0^{\pi} d\theta \int_{\sigma_{LL}}^{\infty} \phi'_{LL}(r)\rho_L r^2 \sin\theta \, dr = -\frac{4}{3}\pi\sigma_{LL}{}^3\epsilon'_{LL}\rho_L \quad (48)$$

Comparing eqs 48 and 6 and considering $\epsilon_{LL} = \epsilon'_{LL}$, one can conclude that $\eta \simeq \sigma_{LL}$. Because the hard core radius σ of liquid−solid interactions can be larger than σ_{LL} (see refs 12, 15, and 16), the ratio σ/η can be larger than unity and cases in which a can acquire values larger than 4 can exist.

The droplet profile depends on the droplet size and on the value of the parameter a. By examining the curvature radius, $R^{curv}(y)$, of the droplet profile, one can see (Figure 5) that for large droplets and $0 < a \leq 4$, $R^{curv}(y)$ is almost constant for all points located at distances y from the solid surface larger than $0.1y_m$, where y_m is the height of the droplet. In such cases, the profile has almost a circular shape. However, for small droplets, $R^{curv}(y)$ changes considerably along the profile and the approximation by a circle is no longer valid.

An interesting transformation of the drop profile occurs for $a > 4$ when the height of the drop approaches the critical value $y_{m,c}$. In this case, the width of the drop becomes much larger than its height and goes to infinity as $y_m \rightarrow y_{m,c}$, and the droplet acquires a pancake shape (see Figure 8) with an almost planar upper boundary.

The microcontact angle of the droplet on the solid surface is always equal to 180°, regardless the values of the other parameters. However, the macroscopic contact angle, defined using a continuation of the circular part of a large droplet, depends on the parameters of intermolecular interactions and densities of the liquid and solid substances. This dependence, as shown in section III.D is in qualitative agreement with experiment.

Acknowledgment. The authors are grateful to Prof. C. J. Radke for providing details regarding the numerical calculations in papers of ref 6. This work was supported by the National Science Foundation.

References and Notes

(1) Ruckenstein, E.; Lee, P. S. *Surf. Sci.* **1975**, *52*, 298.
(2) de Gennes, P. G. *Rev. Mod. Phys.* **1985**, *57*, 827.
(3) Brochard-Wyart, F.; di Meglio, J. M.; Quéré, D.; de Gennes, P. M. *Langmuir* **1991**, *7*, 335.
(4) Widom, B. *J. Phys. Chem.* **1995**, *99*, 2803.
(5) Solomentsev, Y.; White, L. R. *J. Colloid Interface Sci.* **1999**, *218*, 122.
(6) Yeh, E. K.; Newman, J.; Radke, C. J. *Colloids Surf.* **1999**, *156*, 137; **1999**, *156*, 525.
(7) McHale, G.; Newton, M. I. *Colloids Surf.* **2002**, *206*, 79.
(8) Zettlemoyer, A. C. In *Nucleation*; Dekker: New York, 1969.
(9) Nowakowski, B.; Ruckenstein, E. *J. Chem. Phys.* **1992**, *96*, 2313.
(10) Ruckenstein, E. In *Metal−support interactions in catalysis, sintering, and redispersion*; Stevenson, S. A., Dumesis, J. A., Baker, R. T. K., Ruckenstein, E., Eds.; Van Nostrand Reinhold: New York, 1987.
(11) Abraham, F. *Homogeneous Nucleation Theory*; Academic: New York, 1974.
(12) Lee, S. H.; Rossky, P. J. *J. Chem. Phys.* **1994**, *100*, 3334.
(13) Elsgolc, L. E. *Calculus of variations*; Pergamon Press: Addison-Wesley: New York, 1962.
(14) Spelt, J. K.; Li, D.; Neumann, A. W. In *Modern Approaches to Wettability*; Loeb, G. I., Ed.; Plenum Press: New York, 1992; p 101.
(15) Stillinger, F. H.; Rahman, A. *J. Chem. Phys.* **1974**, *60*, 1545.
(16) Martoňàk, R.; Colombo, L.; Molteni, C.; Parrinello, M. *J. Chem. Phys.* **2002**, *117*, 11329.